FED-Vol. 154, Pumping Machinery
ASME 1993

# OBSERVATIONS ON OFF-DESIGN FLOWS IN NON-CAVITATING AXIAL FLOW INDUCERS

**Abhijit Bhattacharyya, Allan J. Acosta, Christopher E. Brennen, and Thomas K. Caughey**
Department of Mechanical Engineering
California Institute of Technology
Pasadena, California

## ABSTRACT

This paper describes an investigation of the flows in unshrouded and shrouded inducers which are known to be highly complex, three dimensional flows with real fluid effects. A flow visualization technique using tufts and paint dots was used to study the flows on the blade, hub and housing at off-design flows. It was found that the blade boundary layer flows were attached to the blade surface and that leakage flows were the cause of the upstream swirling backflow in unshrouded inducers. It was also found that shrouded inducers showed flow reversal near the leading edge in addition to the discharge-to-suction leakage flow. The observations provide a better understanding of the internal flows and the occurrence of upstream backflows.

## NOMENCLATURE

$r_t$ blade tip radius
$\beta$ blade angle
$\varepsilon$ limiting streamline angle
$\phi$ flow coefficient (local axial velocity/tip speed)
$\theta$ tangential direction
$\rho$ density
$\Omega$ rotational speed
$\psi$ head coefficient (static pressure rise/$\rho\Omega^2 r_t^2$)

## INTRODUCTION

'Inducers' are axial flow pump impellers often used at the inlet of conventional pumps to improve their cavitation performance. They are typically used in rocket engine pumps and have various other commercial and aerospace applications. Inducers are characterized by high solidity, large stagger angles and low flow coefficients which enable cavitation bubbles to collapse in the long and narrow passages before they reach the pump (Acosta, 1958 and Lakshminarayana, 1982). Although inducers often have a simple geometry (such as a helical configuration with a constant or varying pitch), it has been found that they have complex, highly three-dimensional internal flows, especially at off-design conditions (Lakshminarayana, 1972). Throughout this paper the term 'off-design' refers to flow coefficients below design.

These internal flows are characterized by viscous real fluid effects which lead to the predominance of the boundary layer flows in the blade passage area. As pointed out by Lakshminarayana (1982), there may be only very small regions where inviscid flow effects are present. It has been stated by Jakobsen (1971) that it is necessary to solve several hydrodynamic problems to obtain an optimum design of an inducer that would provide the required suction specific speed and head rise without introducing undesirable cavitation. These include an understanding of the internal flows in inducers. The complicated flows in inducers along with backflows both upstream and downstream at off-design lead to a drop in efficiency and a high power requirement (Toyokura and Kubota, 1965). There can be other consequences such as the occurrence of large lateral forces at off-design conditions in the presence of downstream asymmetries in the system (Bhattacharyya et. al., 1992). It is therefore important to understand the nature of the internal flows and backflows in inducers. Several researchers, notably Lakshminarayana (1972, 1982) have carried out investigations of these flows. However a complete picture of the internal flows and the mechanism causing the onset

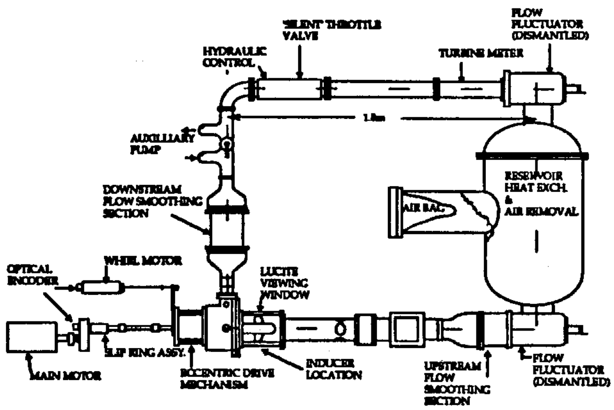


FIG. 1. SCHEMATIC OF THE ROTOR FORCE TEST FACILITY

of upstream and downstream backflows is still not clear.

This paper reports the results of an investigation of these flows in unshrouded and shrouded inducers in water by using flow visualization techniques. It was observed that the blade boundary layer flows were attached to the blade surface and that leakage flows were the cause of the upstream swirling backflow in unshrouded inducers. Shrouded inducers were tested to confirm the origin of the leakage flow and in addition the effect of the shroud on the boundary layer flows. It was observed that shrouded inducers showed flow reversal near the leading edge on the blade which together with the leakage flow exterior to the shroud formed the upstream backflow. The observations revealed further the nature of flows within the inducer and the origin of the upstream backflow.

## EXPERIMENTAL FACILITY AND TEST INDUCERS

The flow visualization experiments were carried out in the Rotor Force Test Facility (RFTF) at the California Institute of Technology. A schematic of the facility is shown in fig. 1 and the reader is referred to Jery (1986) and Franz (1989) for detailed descriptions of the facility. Water is used as the working fluid. The inducer is placed in a transparent lucite housing to enable observations of the flow. The inducers tested were three simple helical inducers with swept leading edges, a constant pitch and hub diameter and blade angles, $\beta_t$, of 9° and 12° for the unshrouded inducers tested and $\beta_t$=12° for the shrouded inducer. The inducer physical characteristics are presented in Table 1. Figure 2 shows the typical geometry of these inducers.

TABLE 1. CHARACTERISTICS OF INDUCERS USED FOR THE EXPERIMENTS

| | UNSHROUDED INDUCERS | | SHROUDED INDUCER |
|---|---|---|---|
| | I | II | |
| Blade angle at tip | 9° | 12° | 12° |
| Blade tip dia. | 10.12 cm | 10.12 cm | 9.71cm |
| Hub/Tip ratio | 0.4 | 0.4 | 0.42 |
| No. of blades | 3 | 3 | 3 |
| Solidity | 1.45 | 1.75 | 1.75 |
| Blade chord | 15.42 cm | 18.57 cm | 17.81 cm |
| Helix lead | 5.04 cm/rev | 6.76 cm/rev | 6.76 cm/rev |
| Blade thickness | 0.15 cm (tip)<br>0.2 cm (root) | 0.15 cm (tip)<br>0.2 cm (root) | 0.15 cm (tip)<br>0.2 cm (root) |
| Shroud thickness | --- | --- | 0.19 cm |
| Shroud length | --- | --- | 5.18 cm |
| Sweep back angle of leading edge (hub to tip) | 69° | 69° | 69° |

## FLOW VISUALIZATION TECHNIQUES

Flow on the inducers and the housing were visualized using tufts and a paint dot technique. Tufts were mounted on the blade surfaces and on the stationary housing. The tufts on the blade surfaces were used to observe the direction of the flow and those on the housing and the hub were used to determine the onset of backflow and swirl on the boundary layer flows. Although the tufts indicate the direction of the relative flow they are unsteady because of the flow and do not clearly indicate whether the flows remain attached on the surfaces because the tuft size and stiffness affects their alignment. In addition, to get a continous picture over the entire surface, several tufts must be used which in turn can cause them to get entangled. In order to overcome these problems, a paint dot method was used to visualize the flow on all surfaces. The technique consists of placing drops of oil paint on the surfaces, about 5mm apart. The paint is mixed with linseed oil to obtain a desired consistency such that the paint (i) does not come off the surface when in stationary water, (ii) does not move due to rotation of the inducer in air at 2000 rpm, (iii) moves primarily due to the shear stress caused in the boundary layer. The inducer is run at a certain flow rate at 2000 rpm for about 5 minutes to allow the paint to flow with the boundary layer fluid. At the end of the run, the paint traces show the direction of the flow (or shear stress) over the blade surfaces, hub and housing. They also indicate the occurrence of separation, if any, from the surface. This method turned out to be very effective.

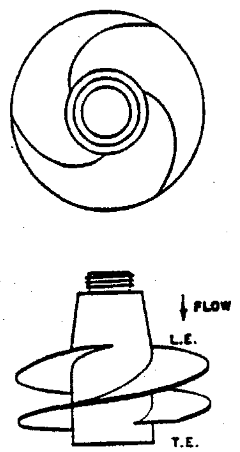


FIG. 2. TYPICAL INDUCER GEOMETRY

TABLE 2A. LIMITING STREAMLINE ANGLES, $\varepsilon$, ON THE SUCTION SURFACE OF THE 12° INDUCER AT $\phi = 0.083$.

| Radial location | Leading edge | Mid-chord | Trailing edge |
|---|---|---|---|
| Hub | 48° | 50° | ~ 70° |
| Mid-radius | 40° | 35° | ~30° |
| Tip | 45° | 29° | 29° |

TABLE 2B. LIMITING STREAMLINE ANGLES, $\varepsilon$, ON THE PRESSURE SURFACE OF THE 12° INDUCER AT $\phi = 0.083$.

| Radial location | Leading edge | Mid-chord | Trailing edge |
|---|---|---|---|
| Hub | 45° | 35° | 30° |
| Mid-radius | 35° | 20° | 25° |
| Tip | 30° | 25° | 25° |

## RESULTS

### Unshrouded Inducers

The boundary layer flows on the blade surfaces and the hub were visualized on unshrouded 9° and 12° inducers, using tufts and paint traces. In the case of the inducers of the type used for the current experiments, it was observed that upstream backflow (observed by tufts on the stationary housing) occurred at ~70% of the design flow and flow reversal downstream (observed by tufts on the hub) occurred at ~60% design flow (in the case of the 9° inducer the design flow is $\phi \approx 0.1$ and a head coefficient $\psi \approx 0.11$). Del Valle et. al. (1991) have also reported the occurrence of the upstream backflow in the 9° inducer by velocity profile measurements.

**Flow on the blade surfaces.** The experiments with the tufts and the paint traces showed the occurrence of increased radial boundary layer flows at off-design flow coefficients on both the suction and the pressure surfaces. The direction of the flow on the leading edge (suction side) had a large radial component, to the extent that the paint traces were almost parallel to the leading edge itself. This is shown in figure 3.

The limiting streamline angle ($\varepsilon$) as defined by Lakshminarayana (1972) have been measured from the paint traces. This is the angle made by the observed streamline on the blade surface relative to the tangential direction and is indicated in figure 4. One typical measurement is shown in the following tables (2) (a) and (b) at a flow coefficient of $\phi = 0.083$ for the 12° inducer. At this flow coefficient, in addition to the upstream backflow, downstream backflow on the hub was also present. While Lakshminarayana (1972) notes a general increase in $\varepsilon$ from the leading edge (LE) to the trailing edge (TE), our experiments find this to be the case only near the hub. However it was observed that aside from the leading edge itself, $\varepsilon$ at the tip does not vary much along the blade (from LE to TE). The value of $\varepsilon$ from mid-chord to the trailing edge on the suction side are high near the hub. In addition, it was noticed that in this region of the blade surface $\varepsilon$ decreases sharply (by about 40°) at about 43% of the blade height. The large $\varepsilon$ near the hub close to the trailing edge is observed when re-entry of flow occurs in the blade passage area.

Visualization on the pressure side also shows large radial boundary layer flows. The values of $\varepsilon$ are lower than those on the suction side (as also reported by Lakshminarayana, 1972). However, our results do not show much variation along the blade chord or along the radius except at the leading edge (where the radial component is large $\varepsilon \approx 70°$).

**Flow on the hub.** The paint dot technique was also used to examine the flow on the hub of the inducer especially in the blade passage region. The flow reverses downstream on the hub and it re-enters the blade passage region as seen by the traces on the hub surface (figure 5). This re-entrant flow continues on the hub until about mid-chord where it meets the fluid from upstream. This interaction causes the hub boundary layer flow to separate in the blade passage area. The paint traces of the re-entrant flow on the hub are also seen to move toward the suction side of the blade.

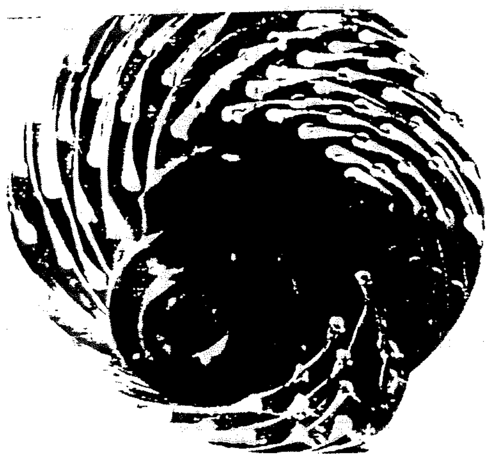

FIG. 3. FLOW ON THE SUCTION SURFACE OF THE 12° UNSHROUDED INDUCER AT $\phi = 0.041$. ROTATION IS IN THE COUNTER CLOCKWISE SENSE AND THE FLOW IS INTO THE PLANE OF THE PAPER.

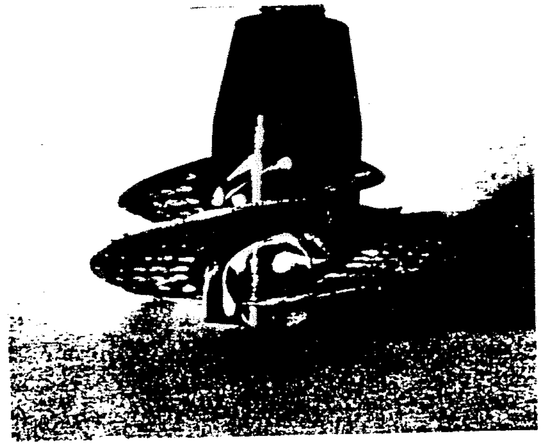

FIG. 5. DOWNSTREAM RE-ENTRY FLOW ON THE HUB (12° UNSHROUDED INDUCER AT $\phi = 0.041$). THE FLOW IS FROM TOP TO BOTTOM AND THE ROTATION IS FROM LEFT TO RIGHT.

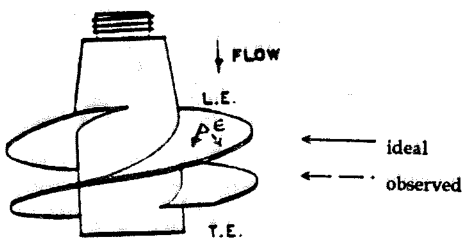


FIG. 4. THE LIMITING STREAMLINE ANGLE ($\varepsilon$).

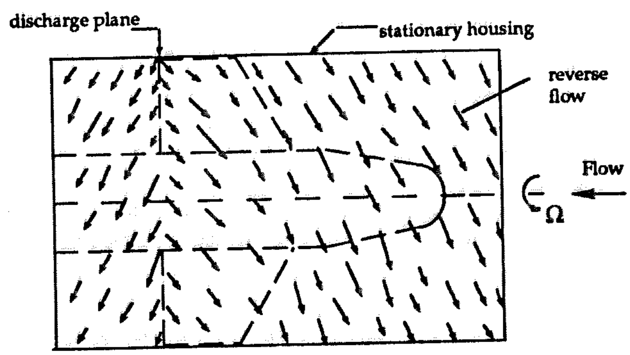


FIG 6. LEAKAGE FLOW ON THE HOUSING INTERIOR (UNSHROUDED INDUCER).

**Flow on the stationary housing.** The flow on the stationary casing around the inducer was also studied using paint dots and tufts. Experiments using tufts confirmed that no leakage flow occurs when the inducer is operated at design or higher flow coefficients. At lower flow rates the tufts reversed direction indicating the presence of leakage flow. The paint traces on the housing represent the time-averaged absolute flow. The experiments revealed that downstream of the discharge plane of the inducer blades, the flow (on the housing) moved downstream along with a tangential component (in the direction of rotation; see figure 6) whereas upstream of this plane the flow moved upstream. This upstream component, in fact, is the reverse flow on the inducer. These experiments revealed the origin of the leakage flow in these axial flow impellers. This aspect is discussed later.

### Shrouded Inducer

A 12° shrouded inducer was also used to visualize internal flow to further investigate the origin of upstream backflow. It also happened that the shroud affected the internal flow to some degree. For example, flow reversal was observed on the suction side of the blade near the tip causing upstream backflow to develop within the inducer (described below). The upstream backflow in shrouded inducers therefore consists of two components: (a) the discharge-to-suction leakage flow exterior to the shroud and (b) the backflow developed within the inducer.

**Flow on the blade surfaces.** The boundary layer flow on the suction side and the pressure side of the blades showed pronounced radial flows in much the same way as in the unshrouded inducers. While the limiting streamline angles could not be measured accurately all across the blade (due to the presence of the shroud), they displayed the same characteristics as the unshrouded inducer, except that at the tip of the blade the values of $\varepsilon$ were close to zero (due to the presence of the shroud). However it was noticed that on the suction side of the blade near the tip, there existed a chordwise location where the flow reversed

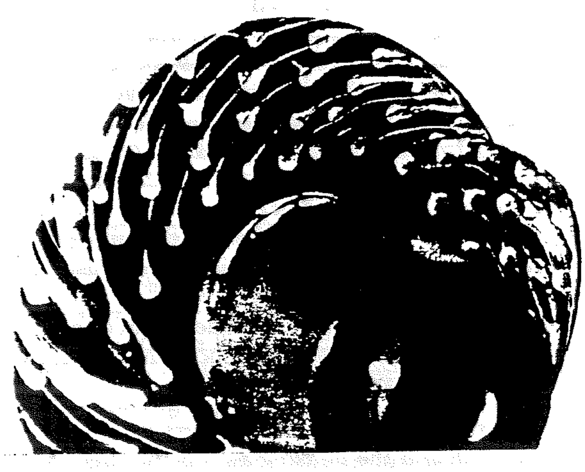

FIG 7. FLOW REVERSAL ON THE SUCTION SIDE OF THE BLADE (SHROUDED INDUCER). ROTATION IS IN A COUNTER CLOCKWISE SENSE.

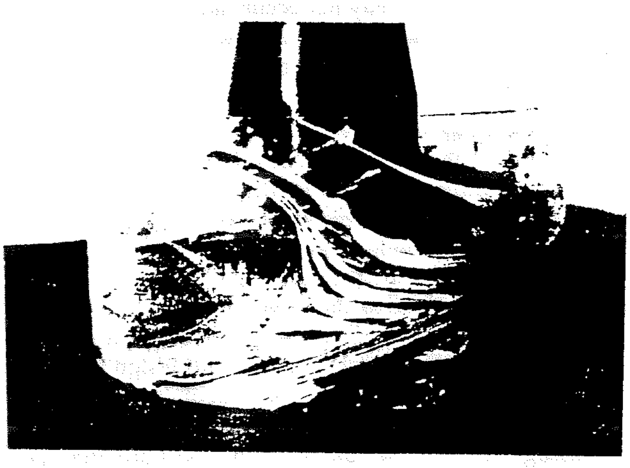

FIG. 8a. FLOW ON THE INTERIOR OF THE SHROUD. THE FLOW IS FROM TOP TO BOTTOM AND THE ROTATION IS FROM LEFT TO RIGHT ($\phi = 0.041$).

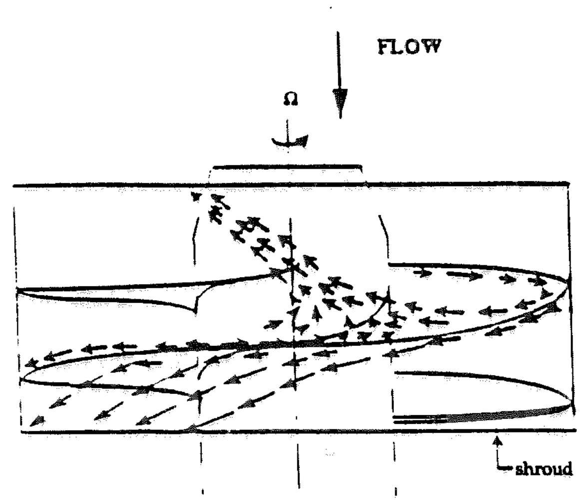


FIG. 8b. SKETCH SHOWING THE FLOW DIRECTIONS FOR FIG. 8a.

direction and started moving upstream near the tip (figure 7).

The reversed flow remains attached to the blade and shroud until it interacts with the fluid from upstream, when it leaves the blade and flows upstream along the interior of the shroud. Upon exiting the shroud, the fluid mixes with the leakage flow exterior to the shroud and forms part of the upstream swirling backflow (figures 8a and 8b).

The reversal point on the suction side of the blade depends on the extent to which backflow has developed and moves closer to the leading edge with decreasing flow rate and increasing backflow. The flow downstream (chordwise) of the reversal point continues to flow downstream. There is no other separation of flow on the blade. The leading edge flow remains attached to the blade surface under all conditions and has a large radial component (as in the case of the unshrouded inducer).

The flow on the pressure side also exhibits a radial component at off-design flow in much the same way as the unshrouded inducer. The radial component of velocity becomes small close to the shroud and is smaller than that on the suction side. Close to the leading edge the flow has a strong radial component of velocity (as in the unshrouded case).

The flow on the hub is similar to that observed for unshrouded inducers. The downstream reverse flow on the hub re-enters the blade passage area and interacts with the upstream flow in the same way as in unshrouded inducers.

Flow on the stationary housing. The leakage flow exterior to the shroud is observed to originate at the discharge end of the rotating shroud. Downstream of this discharge plane, the flow moves downstream and upstream of this plane the flow moves upstream. This upstream component is the discharge-to-suction leakage flow exterior to the rotating shroud. The leakage flow also displays a tangential absolute velocity component in the direction of rotation of the inducer. In addition it is observed that when this leakage flow interacts with the reverse flow generated within the inducer, it results in an increase in the tangential velocity component of the upstream leakage flow.

## DISCUSSION

### Unshrouded Inducers

These experiments have confirmed that the leakage flow between the blades and the housing is indeed the agent of the upstream swirling backflow which was speculated by Acosta (1958) and Del Valle et. al. (1991). The LDA measurements of Howard et. al. (1987) in the blade passage area of an inducer at off-design do not show the presence of reversed flows within the blade passage area. It may be deduced from their results that leakage flows (between blade tip and housing) are the cause of the upstream backflow. Our current experiments have found that the origin of this leakage flow is the discharge plane of the impeller. As the flow rate is reduced, the discharge pressure rises, until at a certain flow rate the adverse pressure gradient causes the low energy radial flow from blade passage to reverse direction in the tip clearance region. That this pressure gradient is indeed the major cause of the leakage flow is verified by the shrouded inducer. Thus the radial component of the velocity at the tip, in the case of unshrouded inducers, promotes this leakage flow. The radial flow may not necessarily be the cause for the leakage flow as has been suggested by Janigro and Ferrini (1973).

The onset of the downstream flow reversal does not seem to be coupled with the upstream reversal as mentioned by Acosta (1992). Acosta (1992) points out the dependence of the onset of upstream and downstream flow reversal on impeller geometry. The work reported by Tanaka (1980), for example, shows this to be true for mixed flow impellers also. Howard et. al. (1987) have shown through their LDA measurements that the near hub axial velocity falls rapidly as the flow rate is reduced, contributing to hub stall. Our observations show that this can occur on the hub close to the trailing edge. The reduction of the axial velocity on the hub at the blade trailing edge together with the strong radial component could create an adverse pressure gradient at the discharge end causing the flow to reverse on the hub and re-enter the blade passage area. The re-entrant flow causes the flow coming from upstream along the hub to separate. This interaction may also be the cause of the secondary vortices in the axial direction observed by Lakshminarayana (1972) by smoke traces near the trailing edge of the inducer.

The existence of the radial component of flow on the blade surface at off-design flows is a well known fact to researchers in this area. Johnston (1970) explains the importance of including centrifugal and Coriolis forces in the analysis of rotating flows. Lakshminarayana (1972) has presented visualization studies indicating the existence of the radial component of the flow on the blades. Furthermore, Lakshminarayana (1978) has demonstrated the 'shear pumping effect', due to the additional head rise caused by the tangential acceleration of the fluid as it moves in a radial path. Lakshminarayana (1978) states that the boundary layers cover the entire passage width and hence radial velocity occurs across the entire passage width.

Our experiments confirm that the flow on the suction side of the blade remains attached (at all off-design flow coefficients). In other words, the separation of flow as reported by investigators (Tanaka, 1980) is not observed by us in axial flow inducers. The limiting streamline angles at the tip of the blade do not vary much along the blade (from LE to TE) due to the interaction of the blade boundary layer with the boundary layer flow on the stationary housing. There is a strong radial component of the blade boundary layer flow near the hub close to the trailing edge. It may be speculated that this radial flow causes the downstream re-entry flow on the hub. The radial component decreases at about mid-blade height due to the interaction with fluid at larger radial locations and due to the effect of the stationary housing.

The interaction of the boundary layers on the blade surfaces, the hub and the housing all together determine the internal flow on the inducer at off-design conditions. From our observations and the above discussion, we may infer that the blade passage area consists of secondary vortices in axial and tangential directions. Near the tip clearance region, the radial flows mix with the strong leakage flow and there may not occur radially inward flow in the blade passage area particularly near the tip.

### Shrouded Inducer

As described above our test results indicate that the upstream backflow observed in the case of a shrouded inducer at off-design flows consists of two components: (a) the discharge-to-suction leakage flow, and (b) separation of flow on the suction surface of the blade. While the leakage flow may be attributed to the adverse pressure gradient exterior to the shroud, the separation at the blades is not due to a change in the angle of attack at off-design flows as has been suggested by Toyokura and Kubota (1968). While the authors do point out that backflow originates inside the flow passage between two blades, they also state that the 'slip of flow' to the pressure side of the blades can be regarded as a phenomenon similar to the separation of flow due to a large increase in the angle of attack. Our observations on the shrouded inducer indicate that the flow on the blade surface is attached on the entire suction surface; the flow reversal at a certain location (along the blade chord) and its subsequent interaction with the upstream flow at blade tip causes the flow to leave the blade surface at the tip and move along the interior of the shroud.

The cause for the flow reversal that occurs on the suction surface of the blade near the tip may be speculated upon. The reversal occurs in a region close to the rotating shroud and is influenced by the shroud boundary layer. Shear forces due to the rotating shroud boundary layer act in a direction opposite to that of the flow in the presence of an adverse pressure gradient. When these shear forces combined with the adverse pressure gradient become larger than the momentum of the fluid (from the shear pumping effect), the flow reverses direction. The flow on the shroud boundary layer within the blade passage area also reverses direction and finally moves upstream.

The internal flow in the shrouded inducer would consist of radially outward flows except near the shroud. On the trailing edge the flows near the hub reverse and the blade passage area would have flows consisting of tangential and axial vorticity components (similar to unshrouded inducers).

## CONCLUSIONS

(1) The flow in the blade boundary layer is attached to the blade surface for unshrouded inducers. The boundary layer flow on the leading edge is almost parallel to the leading edge itself. Limiting streamline angles are high near the leading edge.

(2) Limiting streamline angles are high near the hub especially near the trailing edge. This is accompanied by flow reversal downstream on the hub. These angles decrease close to the blade tip upon interaction with the annullus wall for unshrouded inducers and due to the shroud for shrouded inducers.

(3) The origin of the upstream swirling backflow is at the discharge plane of the inducer for unshrouded inducers.

(4) The discharge-to-suction leakage exterior to the shroud for shrouded inducers originates at the downstream end of the rotating shroud. Flow reversal at the tip near the leading edge, together with the leakage flow constitute the upstream backflow.

(5) Large radial blade boundary layer flows on the suction side occur near the hub close to the trailing edge along with re-entry of the hub boundary layer flow into the blade passage area at off-design conditions.

(6) No radially inward flows were observed at the off-design flows on the blade surfaces. For unshrouded inducers the radially outward flow near the blade tip mixes with the leakage flow and moves upstream.

## ACKNOWLEDGEMENTS

The authors would like to thank the NASA George C. Marshall Space Flight Center for sponsoring the work reported in this paper under grant NAG8-118, technical monitor Henry Stinson. The assistance provided by Asif Khalak in conducting the experiments is also appreciated.

## REFERENCES

Acosta, A.J., 1958, "An Experimental Study of Cavitating Inducers," *Proceedings of 2nd Symposium on Naval Hydrodynamics*, Washington D.C., pp. 533-557.

Acosta, A.J., 1992, "Flow in Inducer Pumps, An Aperçu," *Proceedings of the Fourth International Symposium on Transport Phenomena and Dynamics of Rotating Machinery*, Honolulu, Vol. A, pp. 1-13.

Bhattacharyya, A., Acosta, A.J., Brennen, C.E., and Caughey T.K., 1992, "The Formation of Backflow and its Consequences for Lateral Forces in Axial Flow Pump Impellers," *Abstracts of the ASME Fluids Engineering Conference*, R. Bajura, ed., Los Angeles, FED-Vol. 133, pp.237-239.

Del Valle, J., Braisted, D., M., and Brennen, C., E., 1991, "The Effects of Inlet Flow Modification on Cavitating Inducer Performance," ASME *Journal of Turbomachinery*, Vol.114, pp.360-365.

Franz, R., 1989, "Experimental Investigation of the Effect of Cavitation on the Rotordynamic Forces on a Whirling Centrifugal Pump Impeller," Ph.D. Thesis, California Institute of Technology, Pasadena, CA.

Howard, J.H.G., Tropea, C., Almahroos, H.M.H., and Roeber, T.W., 1987, *Proceedings of the ASME-JSME Thermal Engineering Joint Conference*, P.J. Marto and I. Tanasawa, ed., Honolulu, Vol.2, pp. 63-69.

Jakobsen, J.K., 1971, "Liquid Rocket Engine Turbopump Inducers," NASA Space Vehicle Design Criteria (Chemical Propulsion), R.B. Keller, ed., NASA SP-8052.

Janigro, A., and Ferrini, F., 1973, "Recent Progress in Pump Research," VKI Lecture Series - 61, J. Chauvin, ed., von Karman Institute for Fluid Dynamics, Rhode-Saint-Genése, Belgium.

Jery, B., 1986, "Experimental Study of Unsteady Hydrodynamic Force Matrices on Whirling Centrifugal Pump Impellers," Ph.D. Thesis, California Institute of Technology, Pasadena, CA.

Lakshminarayana, B., 1972, "Visualization Study of Flow in Axial Flow Inducer," ASME *Journal of Basic Engineering*, pp. 777-787.

Lakshminarayana, B., 1978, "On the Shear Pumping Effect in Rocket Pump Inducers," *Pumps,, Analysis, Design and Application*, Worthington Pump Inc., Polytechnic Institute of New York, pp. 49-68.

Lakshminarayana, B., 1982, "Fluid Dynamics of inducers - A Review," ASME *Journal of Fluids Engineering*, Vol. 104, pp. 411-427.

Tanaka, T., 1980, "An Experimental Study of Backflow Phenomena in High Specific Speed Propeller Pump," ASME paper 80-FE-6.

Toyokura, T., Kubota, N., 1965, "Studies on the Improvement of High-Specific-Speed Pump Performance at Low Flow Rates," Bulletin of JSME, Vol.8, No.29, pp.78-88.

Toyokura, T., Kubota, N., 1968, "Studies on Back-Flow Mechanism of Turbomachines: Part 1, Back-Flow Mechanism to the Suction Side of Axial-Flow Impeller Blades," Bulletin of JSME, Vol.11, No.43, pp.147-156.